

A CORE FLOW MODEL OF A HIGH VISCOSITY EMULSION TO DESCRIBE THE BLOOD FLOW IN THE MICROCIRCULATION

Jonas Antonio Albuquerque de Carvalho, jonas.carvalho@gmail.com

Taygoara Felamingo Oliveira

University of Brasília - UnB - Grupo de Mecânica dos Fluidos de Escoamentos Complexos - VORTEX

Francisco Ricardo da Cunha, frcunha@unb.br (Corresponding autor)

University of Brasília - UnB - Grupo de Mecânica dos Fluidos de Escoamentos Complexos - VORTEX

Abstract. The cell-depleted layer in microvessels is of vital importance in the transport of oxygen-saturated red cells to the unsaturated tissues. A high viscosity drop emulsion is used as a theoretical model to describe the blood flow in the microcirculation. We examine the core flow solution with the inner fluid being an emulsion of high viscosity drop facing a small annular gap of Newtonian plasma. A two-equation constitutive model derived from a microstructural approach is applied to describe the behavior of the emulsion flow. The model allows the study of the effect of a number of parameters (capillary number, viscosity ratio and cell volume fraction) on the flow. An intrinsic viscosity of the blood is predicted theoretically as a function of the capillary number and the dimensionless vessel diameter, in agreement with previous experimental studies. The theoretical model suggests that in suspension flows like blood the apparent viscosity may be much reduced by the nonuniform distribution of cells. A possible application of this work could be in illness diagnosis by evaluating of changes in the intrinsic viscosity due to blood abnormalities.

Keywords: Blood rheology, red cell, blood intrinsic viscosity, microcirculation, Fahreaus-Lindqvist.

1. INTRODUCTION

The red cell and plasma properties are significantly altered in many diseased states. The microcirculation is the site where the earliest manifestations of cardiovascular disease (in particular, inflammatory processes).

Blood is a concentrated suspension of red cells, white cells and platelets in plasma. The plasma has approximately the same density $1000\text{kg}/\text{m}^3$ and viscosity 0.001Pas as water. The average volume fraction of red cells (i.e. hematocrit) in the human body is about 40-45% although it may vary considerably within the microcirculation (Pries *et al.*, 1994). The volume fraction of white cells is less than 1% and platelets occupies an even smaller volume fraction. Thus, the rheology of blood is primarily determined by red cells (Skalak *et al.*, 1989). In microvessels of $7\mu\text{m}$ in diameter or less, the red cells deforms and organize in lines (see Fig. (1a)). A thin film of plasma of $0.5 - 1.0\mu\text{m}$ thickness (Lipowsky, 2005), separates the cell membrane from the capillary wall. The blood rheology in such capillaries are critically determined by the clearance between the cell and endothelial wall (see review by Fung, 1973). Secomb *et al.*, 1986, exploited the fact that lubrication theory applies in this case, and solved for velocity and shape of a red cell centered in a uniform cylindrical capillary.

The pictures 1b, 1c in Fig. (1) show different dimensional regimes of the cell motion in microvessels. Fortunately, and approximative description of non-axisymmetric red cell motion in micro-vessels suggests that tank-treading motion has little rheological effect (Secomb and Hsu, 1996).

The cell-depleted plasma layer that forms adjacent to vessel walls is an important example of the behavior of the blood

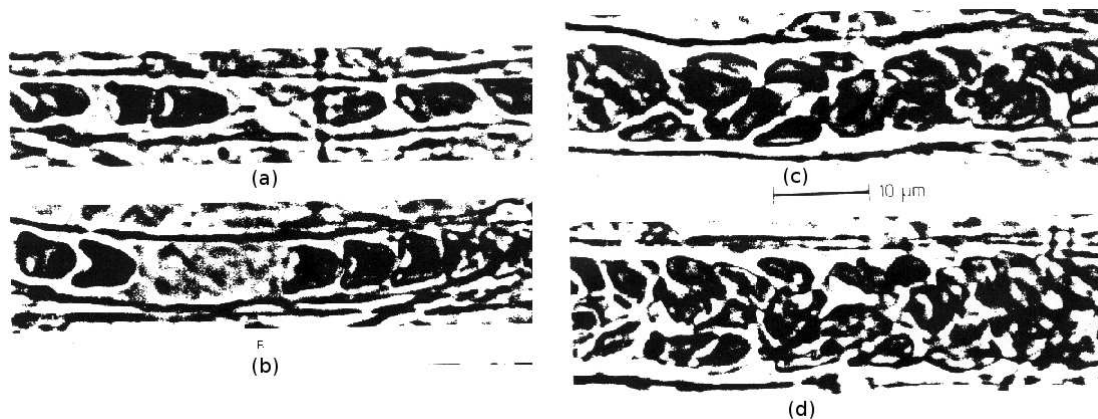


Figure 1. Illustration of red cells flow in capilar of diameter less then 7μ .

in microvessels. The Fahraeus and Fahraeus-Lindqvist effects (Fahraeus, 1929; Fahraeus and Lindqvist, 1931) are the classical manifestations of the cell-depleted layer in micro-vessels. The first describes the reduced hematocrit in vessels less than 0.3mm in diameter. Fahraeus (and many subsequent investigators) performed experiments with blood flow in long glass tubes discovering that the tube hematocrit measured by stopping the flow and emptying the tube content was consistently smaller than the discharge hematocrit measured in the discharge reservoir. The second effect describes the concomitant reduction in flow resistance with the decrease of the intrinsic viscosity. It reaches a minimum at diameter vessels of approximately $5\mu m$. After this minimum the blood apparent viscosity increases as tube diameter decrease. This inversion of the Fahraeus-Lindqvist effect corresponds to the regime in which the red blood cells move in single-line flow (see illustration of this regime in Fig. (1)).

Approximately 80% of the total pressure drop between the aorta and the vena cava occurs in micro-vessels (Popel and Jonhson, 2005). The presence of a cell-depleted layer near the vessel wall in blood flow promotes the *skimming plasma* that has a significant effect on the pressure drop needed to drive blood flow through the smaller vessels.

Red blood cells have approximately $90\mu m^3$ of volume and $135\mu m^2$ of surface area. In the absence of deformation-inducing flow, red cells assume a biconcave disk-shape of approximately $8\mu m$ and $2\mu m$, that is, disks with a double-sided dimple at the center (see Fig. (2)). Red cells suspended in plasma are neutrally buoyant.

Basically, the blood assume three different regimes. For diameters of 0.6 to 1mm the blood still have a homogenous aspect. The red blood cells has uniform distribution and the blood intrinsic viscosity is independent of the vessel diameters size. For healthy person it has a value of 3.0mPas (Cunha, 2002). In the range of 0.02 to 0.6mm the red blood cells occupy central region of the blood vessel, and a cell-depleted plasma layer with thickness $\delta = 2\mu m$ appears. For vessels with diameter up few cell size, the cells travel in single-line (Secomb, 2005). The dynamics is dominated by cell-wall interactions and the rheology of the blood can be accurately predicted by considering the motion of a single red cell. In this regime non-continuum effects of the blood arises from the finite size of the red blood cells and a description of the blood as a homogenous fluid should not be applied.

Red blood cells, of a mammalian, consist of a thin flexible membrane containing the cytoplasm: an aqueous solution of hemoglobin that behaves as a Newtonian fluid with a viscosity several times larger than the plasma, $\mu_i \sim 10^{-2}Ns/m^2$. The cytoplasm fluid is incompressible; thus, cell volume is preserved. The red cell membrane exhibits viscoelastic properties (Evans and Skalak, 1980) that have been extensively studied (Popel and Jonhson, 2005). According to theses studies, the mechanical properties of the red cell membrane are characterized by four material constants; an elastic modulus of dilatation $E_D = 0.5N/m$, an elastic modulus of shear $E_S \sim 6 \times 10^{-6}$, a bending moment $M_B \sim 2 \times 10^{19}Nm$ and shear viscosity $\mu_{\dot{\gamma}} = 10^{-6}Ns/m$. The large magnitude of E_D indicates that the area of a red cell membrane remains essentially constant.

In this paper the cell-depleted layer is modeled as a plasma layer in a core flow with a dilute emulsion with drops of high viscosity ratio working as prototypes of red blood cells. The emulsion will represent the concentrated blood that travels in the core region of micro-vessels with a plasma skimming effect due to the cell-depleted layer adjacent to the wall. The emulsion model has reproduced the shear thinning behavior of the blood due to the deformation of the prototypes cells. In addition, we compute the viscosity decrease with vessel diameter and the effect of the viscosity ratio and hematocrit on the intrinsic apparent viscosity of blood. This model in comparison with experimental results of in vivo experiments shows a qualitative good agreement and evidences the absence of some blood properties as cell aggregation.

1.1 A Dimensional Analysis

In this subsection some scaling arguments are presented in order to identify the main physical parameter to show that the flow in the microcirculation is characterized by a low-Reynolds number flow (Cunha, 2002). We use typical physiological pressure gradient of $\Delta p = 60mmHg$ over $l = 1cm$ in the microcirculation. The plasma has approximately the same density $\rho \approx 1000Kg/m^3$ and viscosity $\mu_p \approx 0.001Ns/m^2$ as water. The Poiseuille's law for the flow in a micro-vessel of radius $100\mu m$ provides an estimate of the local shear rate $\dot{\gamma} = R\Delta p/(8\mu_p l) \sim 10^4s^{-1}$. On the length

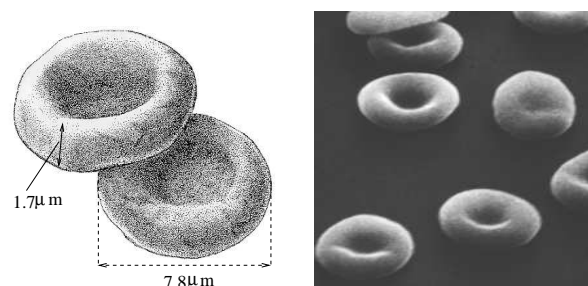


Figure 2. Illustration of the biconcave shape of non-deformed erythrocytes and their typical (dimensions in the absence of deformation)

scale of a red cell, $a = 5\mu m$, the Reynolds number that characterizes the plasma flow is $Re = \rho\dot{\gamma}a^2/\mu_p \sim 0.1$. The results indicates that viscous stresses dominate the inertial stresses in the plasma. Now, using the physical constants that characterize the mechanical properties of red cells, we can form the group of dimensionless parameters shown in Tab. (1).

Table 1. Dimensionless physical parameters of the cells motion in microvessels. The parameters are from physiologic normal erythrocytes in microvessels.

Dimensionless parameter	Physical meaning	Value
Membrane viscosity ratio: $\lambda_m = \frac{\mu_m}{\mu}$	Relative importance of membrane viscosity	$\lambda_m \sim 300$
Cytoplasmatic viscosity ratio: $\lambda_i = \frac{\mu_i}{\mu}$	Relative importance of cytoplasmatic flow	$\lambda_i \sim 10$
Elastic capillary parameter: $Ca_S = \frac{\mu\dot{\gamma}a}{E_S}$	Viscosity and elastic stresses ratios	$Ca_S \sim 0.5$
Bending parameter: $C_B = \frac{\mu\dot{\gamma}a^3}{M_B}$	Viscous and bending stresses ratio	$C_B \sim 100$
Dilatation parameter: $C_D = \frac{\mu\dot{\gamma}a}{E_D}$	Dilatation and viscous stress ratio	$C_D \sim 10^{-5}$

The typical parameter values displayed in the table above are obtained from the well-established mechanical properties listed in §1 and the local shear has been estimated in this section.

A number of important conclusions can be drawn on the basis of the dimensionless parameter defined above. The small magnitude of C_D indicates that viscous stress are too small to significantly dilate the red cell membrane; the surface are of a red cell remains essentially constant, as expected. The observations that $\lambda_i \ll \lambda_m$ indicates that membrane viscosity dominates the cytoplasmic viscosity. Thus, the internal circulation of the cytoplasm is largely masked by the membrane viscosity and is expected to have little dynamical effect on red cell motion. This prediction is in agreement with theoretical studies (Barthes-Biesel and Sgaier, 1985; Secomb and Hsu, 1996) Actually this property has also motivated the present work when considering an emulsion of high viscosity ration dropas a first proptotype model for the. The estimative that $Ca_S = O(1)$ indicates that the elastic shear stresses are significant, as expected. The bending parameter is large suggesting that bending stress are unimportant. However, bending stresses should be estimated from the curvature radius of the red cell membrane. Thus, we could re-define the parameter $C_B = \mu_p\dot{\gamma}/M_B\kappa^3$, where κ is a typical curvature. For a deformed red cell, κ may be several times larger than $1/a$ thus, $C_B = O(1)$ indicating that bending stresses are important. This finding is in agreement with predictions of Secomb *et al.*, 1986. In summary our dimensional analysis predicts that red cell motion in the micro-vessels is constrained by constant area and is sensitive to three parameters: the membrane viscosity ratio μ_m , the elastic capillary parameter Ca_S , and the bending parameter, C_B .

2. PRESSURE DRIVEN CORE FLOW IN MICRO VESSELS

In this section we consider a model of a core flow emulsion of high viscosity ratio in order to examine the pressure-driven flow of blood in micro-vessels. The drops of high viscosity as compared to the plasma viscosity, in the present context are prototypes of the red cells. It is used a dilute theory to calculate the influence of each cell prototype alone to the main flow. The present model has permitted to evaluate the intrinsic blood viscosity function of the capillarity number, the viscosity ratio and the cells volume fraction. The dilute emulsion occupies the core region of the micro-vessel whereas a plasma layer occupies the region adjacent to wall. A schematic of the problem is shown in comparison with a micro-vessel micrographic in Fig. (3).

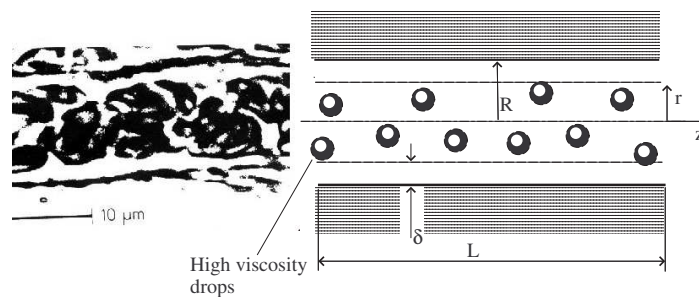


Figure 3. Typical micro-vessel with approximated $10\mu m$ of diameter. The blood emulsion travels in the core of the vessel whereas a thin cell-depleted layer (with thickness δ) containing pure plasma flowing adjacent to the wall.

2.1 Governing Equations

The general equations of conservation of mass and momentum for the flow illustrated in Fig. (3) are described next. For the thin cell-depleted layer containing pure plasma, applies following balance equation

$$\nabla \cdot \mathbf{u} = 0, \quad -\nabla p + \nabla \cdot \boldsymbol{\tau}^* = 0. \quad (1)$$

The plasma is considered an incompressible Newtonian fluid of viscosity μ_p , and the constitutive equation for the stress tensor $\boldsymbol{\tau}^* = 2\mu_p \mathbf{D}$. Here \mathbf{u} represents the Eulerian velocity field, p is the pressure and $\mathbf{D} = 1/2(\nabla \mathbf{u} + \nabla \mathbf{u}^T)$ denotes the rate of strain tensor of the flow.

For the blood emulsion in the core flow region ($0 \leq r^* \leq R - \delta$) the governing equation describing the balance of mass and momentum are respectively given by

$$\nabla \cdot \mathbf{u} = 0, \quad -\nabla p + \nabla \cdot \boldsymbol{\sigma}^* = 0, \quad (2)$$

where

$$\boldsymbol{\sigma}^* = 2\mu_p \mathbf{D} + \boldsymbol{\Sigma}^d. \quad (3)$$

The blood emulsion is modeled as a high viscosity ratio dilute emulsion ($\lambda \gg 1$) and the drop contribution to the stress tensor are calculated by $\boldsymbol{\Sigma}^d$, expressed as (Oliveira, 2007)

$$\boldsymbol{\Sigma}^d = 2\tilde{\mu}(\lambda, \phi) \mathbf{D} + \frac{4}{Ca} \mathbf{A} + \frac{15}{7} \left[\mathbf{A} \cdot \mathbf{D} + \mathbf{D} \cdot \mathbf{A} - \frac{2}{3} (\mathbf{A} : \mathbf{D}) \mathbf{I} \right], \quad (4)$$

where $\tilde{\mu} = \phi[5/2 - 25/(4\lambda)]$, ϕ is the cell volume fraction, λ is the viscosity ratio between the drop and plasma, $Ca = \lambda \mu \dot{\gamma}_c a / c$, $c = 20/19$. The distortion tensor \mathbf{A} is determined by a particular case of the Frankel and Acrivos, 1970 and Oliveira, 2007.

$$\frac{d\mathbf{A}}{dt} = Ca \mathbf{W} \cdot \mathbf{A} - Ca \mathbf{A} \cdot \mathbf{W} + \frac{5}{2\lambda} Ca \mathbf{E} - c \mathbf{A}, \quad (5)$$

where \mathbf{W} is the anti-symmetric part of the velocity gradient (vorticity tensor). Note that the absence of the drops in the flow $\boldsymbol{\Sigma}^d = \mathbf{0}$ corresponding to a flow of pure plasma and the core region is full of plasma with $\boldsymbol{\tau} = 2\mu_p \mathbf{D}$.

2.2 Solution Of The Core Axisymmetric Emulsion Flow In A Tube

In this section the solution for the velocity profile and its associated flow rate and the intrinsic viscosity of the blood based on the two-phase model will be presented. As mentioned before the dilute emulsion of high viscosity drop occupies the core region defined by the domain $0 < r \leq \xi$, where r is a dimensionless radius defined as $r = r^*/R$ and ξ is the dimensionless ratio $\xi = (R - \delta)/R$. The annular region (See Fig. 3), occupied by pure plasma defines the domain $\xi < r < 1$. We suppose a isothermal flow in steady state and the drops density differ only slightly from that of plasma, so that the buoyancy effects are neglected. In the present formulation cylindrical coordinates are used and the vessel wall has a constant radius R . The pressure gradient is then constant along the dimensionless coordinate z .

The complete set of governing equations described in §2.1 written in terms of cylindrical coordinates takes the form

$$\begin{cases} \frac{1}{r} \frac{\partial}{\partial r} (r\sigma) = -ReG & \text{for } 0 < r \leq \xi \\ \frac{1}{r} \frac{\partial}{\partial r} (r\tau) = -ReG & \text{for } \xi < r \leq 1 \end{cases} \quad \text{and its solution} \quad \begin{cases} \sigma = -\frac{ReG}{2} r & \text{for } 0 < r \leq \xi \\ \tau = -\frac{ReG}{2} r & \text{for } \xi < r \leq 1 \end{cases}. \quad (6)$$

where $\tau = \tau^*/U/R\mu_p$, $\sigma = \sigma^*/U/R\mu_p$, $G = (\partial p/\partial z)/\rho U^2$ where U is the average velocity of the flow and the variables with the notation (*) are dimensional quantities. In addition, according to Fig. (3) the imposed boundary conditions are the non-slip boundary on the vessel-wall (no porous vessel), the symmetry condition on the axis of the tube (i. e. no shear stress) and velocity and stress continuity on the interface between the blood emulsion and cells depleted layer. These conditions are written as follows

$$\sigma(0) = 0, \quad u_p(1) = 0, \quad \sigma(\xi) = \tau(\xi), \quad u_s(\xi) = u_p(\xi) \quad (7)$$

where u_s and u_p means respectively the velocity profile in the blood domain (core region) and velocity profile in the plasma domain (adjacent layer to wall). The contour conditions are used to calculate the solution of the governing equation in Eq (6).

Now, substituting Eq. (3) into Eq. (6) with the definition of Σ^d , given by Eq. (4), and the steady solution of \mathbf{A} from Eq. (5), the following set of differential equation in cylindrical coordinates are determined.

$$\left\{ \begin{array}{l} \mu_T \frac{du}{dr} + \epsilon \left[\mu_B \left(\frac{du}{dr} \right)^3 + \frac{GRe}{2} r \left(\frac{du}{dr} \right)^2 \right] = -\frac{GRe}{2} r \quad \text{for } 0 < r \leq \xi \\ \frac{du}{dr} = -\frac{GRe}{2} r \quad \text{for } \xi < r \leq 1 \end{array} \right. \quad (8)$$

where $\mu_T = 1 + \phi[5/2 + 3/(2\lambda)]$ (Taylor's viscosity, (Taylor, 1932) associated to the limit $ca \ll 1$), $\mu_B = 1 + \tilde{\mu}$ (Blob viscosity, associated to the limit $Ca \gg 1$), $\epsilon = (aCa/cR)^2$.

Solving the velocity field in the core region in the Eq. (8) simply gives the parabolic profile

$$u_p(r) = -\frac{ReG}{4}r^2 + E. \quad (9)$$

In order to calculate the integration constant E , we apply the non-slip condition $u_p(1) = 0$ and thus we find for the velocity profile in this region the following expression

$$u_p(r) = \frac{ReG}{4}(1 - r^2). \quad (10)$$

In Eq (8) we propose for the solution of the differential equation in the blood emulsion side a regular perturbation method based on the small parameter ϵ . The velocity field in the core region is then expressed as

$$u_s(r) = u_0(r) + u_1(r)\epsilon + u_2(r)\epsilon^2 + \dots = u^p(r) + u'(r). \quad (11)$$

A similar perturbation method have been used by Cunha and Sobral, 2004 in the context of pressure driven flow of magnetic fluids. Note that this velocity profile may be the summation of a parabolic profile that is $u^p(r)$ and a non-parabolic profile $u'(r)$ due to the presence of high viscosity ratio drops. Using Eq. (11) in the differential equation of the core domain of Eq. (8) we can find, for terms with ϵ^0 , the following differential equation

$$\mu_T \frac{du_0}{dr} + \frac{ReG}{2}r = 0. \quad (12)$$

For terms with ϵ^1 we can find

$$\mu_T \frac{du_1}{dr} + \mu_B \left(\frac{du_1}{dr} \right)^3 + \frac{1}{2}GRe \left(\frac{du_0}{dr} \right)^2 = 0. \quad (13)$$

For those with ϵ^2 there is

$$\mu_T \frac{du_2}{dr} + 3\mu_B \left(\frac{du_0}{dr} \right)^2 \left(\frac{du_1}{dr} \right) + GRe \left(\frac{du_0}{dr} \right) \left(\frac{du_1}{dr} \right) = 0. \quad (14)$$

The respectively solutions for u_0 , u_1 and u_2 are

$$u_0(r) = -\frac{1}{4} \frac{GRe}{\mu_T} r^2 + A_0, \quad u_1(r) = -\frac{G^3 Re^3 (\mu_T - \mu_B)}{32\mu_T} r^4 + A_1, \quad u_2(r) = -\frac{Re^5 G^5 (\mu_T - \mu_B)}{2\mu_T - 3\mu_B} 192\mu_T^7 r^6 + A_2. \quad (15)$$

The continuity velocity contour condition $u_p(\xi) = u_s(\xi)$ condition is used to calculate each integration constant A_0 , A_1 and A_2 . This condition states that in the blood-plasma interface the blood velocity profile is then a parabolic profile and independent of ϵ . Then we solve the following equations

$$u_0(\xi) = u_p(\xi), \quad u_1(\xi) = 0 \quad \text{and} \quad u_2(\xi) = 0 \quad (16)$$

and find

$$A_0 = \frac{1}{4}GRe \left(1 - \xi^2 + \frac{\xi^2}{\mu_T} \right), \quad A_1 = \frac{G^3 Re^3 (\mu_T - \mu_B)}{32\mu_T} \xi^4, \quad A_2 = \frac{Re^5 G^5 (\mu_T - \mu_B)}{2\mu_T - 3\mu_B} 192\mu_T^7 \xi^6. \quad (17)$$

And the resulting blood velocity profile is expressed as

$$u_s(r) = \frac{ReG}{4} \left[1 - \xi^2 + \frac{1}{\mu_T} (\xi^2 - r^2) \right] + \frac{G^3 Re^3 (\mu_T - \mu_B)}{32\mu_T} (\xi^4 - r^4) \epsilon + \frac{Re^5 G^5 (\mu_T - \mu_B)}{2\mu_T - 3\mu_B} 192\mu_T^7 (\xi^6 - r^6) \epsilon^2 \quad (18)$$

Note that if the drop volume fraction tends to zero ($\phi \rightarrow 0$), the blood velocity profile tends to the plasma layer velocity profile.

3. Intrinsic Viscosity

In this section we solve the flow and calculate the intrinsic viscosity of the blood. It is calculated by the equality of the core flow and a Poiseuille law with the intrinsic viscosity μ_s as follows

$$\pi R^2 U = \frac{\pi R^4}{8\mu_s} G \frac{\rho U^2}{R}. \quad (19)$$

The Eq. (19) results in the dimensionless intrinsic viscosity, expressed as

$$\frac{\mu_s}{\mu_p} = G \frac{\rho R U}{\mu_p 8} = \frac{ReG}{8}. \quad (20)$$

The dimensionless core flow is calculated by the integral

$$\frac{\tilde{Q}}{\pi} = \int_0^1 2u(r)rdr = \int_0^\xi 2u_s(r)rdr + \int_\xi^1 2u_p(r)rdr, \quad (21)$$

that results in the following expression

$$\frac{\tilde{Q}}{\pi} = \frac{ReG}{8} f_1 + \left(\frac{ReG}{8}\right)^3 f_2 \epsilon + \left(\frac{ReG}{8}\right)^5 f_3 \epsilon^2, \quad (22)$$

where

$$f_1 = \frac{\xi^4}{\mu_T} - \xi^4 + 1, \quad f_2 = \frac{32}{3\mu_T^3} \left(1 - \frac{\mu_B}{\mu_T}\right) \xi^6, \quad f_3 = \frac{128}{\mu_T^5} \left(2 - 5\frac{\mu_B}{\mu_T} + 3\frac{\mu_B^2}{\mu_T^2}\right) \xi^8. \quad (23)$$

Since the dimensionless flow $\tilde{Q} = \pi$, the intrinsic viscosity is the solution of the following equation

$$\frac{\mu_s}{\mu_p} f_1 + \left(\frac{\mu_s}{\mu_p}\right)^3 f_2 \epsilon + \left(\frac{\mu_s}{\mu_p}\right)^5 f_3 \epsilon^2 - 1 = 0 \quad (24)$$

To solve the Eq. (24) we use an iterative method of the successive substitutions described in (Hinch, 1997) with the recursive equation expressed as

$$\mu_{i+1} = \frac{1}{f_1} \mu_i - (\mu_i)^3 \frac{f_2}{f_1} \epsilon + (\mu_i)^5 \frac{f_3}{f_1} \epsilon^2. \quad (25)$$

where μ_i are dimensionless terms, given by

$$\mu_1 = \frac{1}{f_1}, \quad \mu_2 = \frac{1}{f_1} - \frac{f_2}{f_1^4} \epsilon, \quad \mu_3 = \frac{1}{f_1} - \frac{f_2}{f_1} \left(\frac{1}{f_1} - \frac{f_2 \epsilon}{f_1^4}\right)^4 \epsilon - \frac{f_3}{f_1} \left(\frac{1}{f_1} - \frac{f_2 \epsilon}{f_1^4}\right)^5 \epsilon^2. \quad (26)$$

resulting in the following closed expression for the intrinsic viscosity

$$\frac{\mu_s}{\mu_p} = \frac{1}{f_1} - \frac{f_2}{f_1^4} \epsilon + \left(\frac{3f_2^2}{f_1^7} - \frac{f_3}{f_1^6}\right) \epsilon^2 \quad (27)$$

4. NUMERICAL SOLUTION

In this section the core flow governing equation are solved numerically. Once numerical solution is validated by the asymptotic solution presented in §3. the intrinsic viscosity may be evaluated in more extreme regime of the flow. In other words the parameter ϵ is not necessarily small.

First, a Newton-Raphson method is used in Eq. (8) to calculate

$$f(r) = \frac{du}{dr} \quad (28)$$

Using two Taylor expansions of the velocity profile, about $-\Delta r$ and Δr , for central finite difference, we find

$$u_{i+1} - u_{i-1} = 2\Delta r \frac{du}{dr}(r_i) = 2\Delta r f(r_i). \quad (29)$$

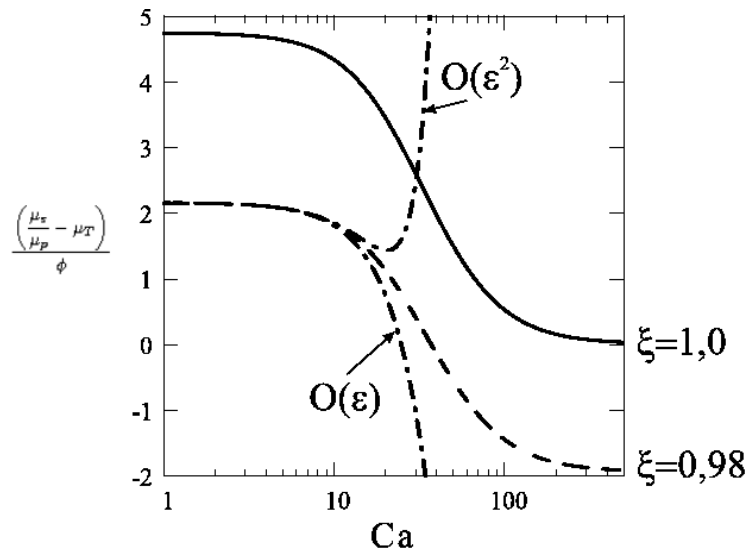


Figure 4. Dimensionless intrinsic viscosity of blood as a function of the capillary number for two values of ξ . Solid line represents $\xi = 1.0$, dashed line $\xi = 0.98$

where i is an iteration index. Now Eq. (29) results in a set of n algebraic equations with a three-diagonal coefficient matrix namely

$$\begin{bmatrix} 0 & -1 & 0 & 0 & 0 & \dots & 0 \\ 1 & 0 & -1 & 0 & 0 & & 0 \\ 0 & 1 & 0 & -1 & 0 & & 0 \\ \vdots & & & & \ddots & & \\ 0 & \dots & 0 & 0 & 0 & 1 & 0 \end{bmatrix}_{n \times n} \cdot \begin{Bmatrix} u_1 \\ u_2 \\ u_3 \\ \vdots \\ u_n \end{Bmatrix} = \begin{Bmatrix} 2\Delta r f(r_1) \\ 2\Delta r f(r_2) \\ 2\Delta r f(r_3) \\ \vdots \\ 2\Delta r f(r_n) \end{Bmatrix} \quad (30)$$

The system in Eq. (30) has been solved by a self contained Compaq Visual Fortran 6.0 code to solve three-diagonal matrixes systems that results in the velocity profile of the flow u_i . The dimensionless flow \tilde{Q} is then calculated by a trapezoidal numerical integration.

In order to evaluate the intrinsic viscosity of the flow numerically we define the function:

$$G(Re) = \tilde{Q} - \pi \quad (31)$$

Using a Newton-Raphson iterative method to calculate the parameter ReG , say

$$Re_{new} = Re_{old} - \frac{G(Re)}{G'(Re)}, \quad (32)$$

The new Reynolds number is calculated and the flow is solved in a loop until $|Re_{old} - Re_{new}| < Tol$, where tol is a tolerance of 10^{-3} and the dimensionless intrinsic viscosity is calculated by the expression of Eq. (20)

5. RESULTS

The model based on a high viscosity dilute emulsion predicts satisfactory a shear thinning behavior of the blood. The deformation and orientation in the flow direction of the prototypes cells cause the decreasing of the intrinsic viscosity. *In vitro* experiments show that 75% of the viscosity decrease is a result of the hemolysis of red cells aggregation where 25% is due to the red cell deformation in response to increase shear stress (Lipowsky, 2005). Figure (4) shows the plot of the dimensionless intrinsic viscosity of blood as a function of the dimensionless shear rate (i. e. Capillarity number). The lower dashed curve represents the core flow numerical solution with a cell-depleted layer of $\delta/R = 0.02$ and the higher solid curve is the solution without the plasma layer (i. e. $\delta/R = 0$). The dashed-dots curves are the asymptotic solutions witch are in good agreement with numerical solution for $Ca < 20$. The lower viscosity of the core flow in comparision with the fulfilled emulsion tube states a skimming effect due to the presence of the plasma layer observed by in experimental results (Sutera and Skalak, 1993).

As Fahraeus and Lindqvist, 1931 pointed out the viscosity of blood decrease with the micro-vessel diameter (Pries *et al.*, 1992). Actually the core flow model proposed explored has shown blood viscosity decreasing $R/\delta < 50$. Experimental data in long tubes with diameter less than $300\mu m$ show precipitous decrease in intrinsic viscosity (Popel and

Jonhson, 2005). This behavior decrease the heart pump work to win the pressure difference in microcirculation which correspond 80% of the pressure difference between the aorta and vena cava (Popel and Jonhson, 2005). Figure (5) shows the decrease of the intrinsic viscosity of flow solution as a function of the dimensionless radius R/δ . The dashed curve represents in the core region a dilute emulsion of high viscosity ratio with 30% of volumetric fraction, the and the dots are the viscosity law fit from Pries *et al.*, 1994, of *in vivo* observations 30% of hematocrit.

The difference between the viscosity law and the emulsion core flow prediction is approximated 20%. This difference can be explained by the absence of vessel wall irregularities, witch is markable in the blood flow and increase the blood viscosity substantially.

At the low level of microvascular hematocrit found in most tissues in the normal flow state, the intrinsic viscosity varies linearly with microvessel hematocrit (Lipowsky *et al.*, 1980). The emulsion core flow solution presented shows a close linear relation $\mu_s/\mu_p \times \phi$ in Fig. (6). This result can be used to estimate the intrinsic viscosity of blood due to abnormal hematocrit in blood with pathology. It is important to emphasize that the emulsion core flow solution do not predicts the intrinsic viscosity behavior with the drop volume fraction $\phi > 0.3$ with accuracy due to the dilute theory. Figure (6) shows however a good qualitative agreement between the prediction and experimental results in vitro for $\phi < 40$.

In red cells, the parameter λ is related to the cytoplasm and membrane structures, i. e. related to λ_m of Tab. (1), which define the deformability of the cell. As exposed in §1.1, λ_m is a significant physical parameter to the microcirculation rheology. The emulsion core flow solution presented in this article shows approximated null variation of intrinsic viscosity for values $\lambda > 20$. For values of $\lambda < 20$ the intrinsic viscosity decrease with λ . Pathologies such as genetic alterations in cytoplasm, and inadequate ATP supply to support the ion transport systems may result in abnormal λ once these

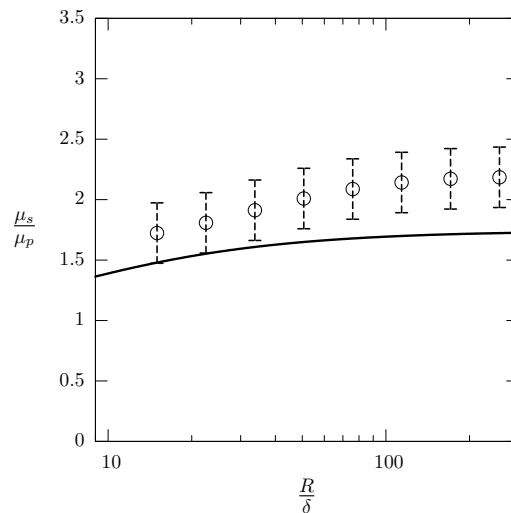


Figure 5. Dimensionless intrinsic viscosity of the blood as a function of the aspect ratio R/δ for the different hematocrit. Open circle are in vivo experimental observations with hematocrit of $\phi = 0.3$ and error of 0.25. The solid line is the core flow numerical results for volume fraction of $\phi = 0.3$.

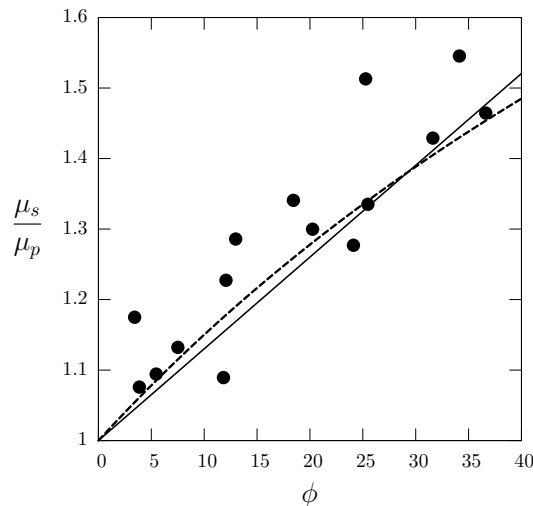


Figure 6. Intrinsic blood viscosity as a function of the cell volume fraction (Hematocrit). Dashed line represent the core flow model results, the solid line a linear fit and black fill circles are experimental results.

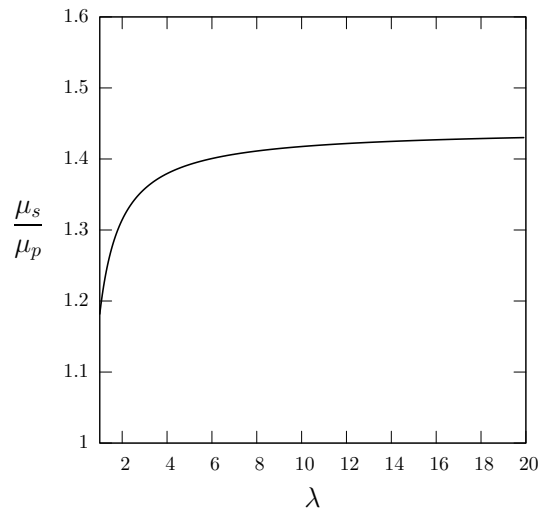


Figure 7. Dimensionless intrinsic viscosity as a function of the viscosity ratio between cell prototypes and plasma

pathologies lead to abnormal deformability of cells (Chien, 1987, Mohandas and Evans, 1998, Mohandas and Shohet, 1981). The result, with experimentation, may help in calculate an estimated intrinsic viscosity of a blood with pathologies that leads to $\lambda < 20$. It is important to remember that the adopted theory consider a low deformable cell prototype, i. e. $\lambda > 1$.

6. CONCLUSION

The core flow of high viscosity emulsion shows a shear thinning behavior starting in $Ca \approx 10$. In the present model, the deformation of cell prototypes are the only mechanism to provoke the shear thinning, as long cells aggregation due to the proteins composition of plasma are neglected.

The plasma skimming layer of thickness 2% of microvessel radius decrease the intrinsic viscosity for any Capillarity number in comparison of a fulfilled tube with emulsion. It leads to newtonian limits in low Capillarity number and infinity capillarity under the Taylor viscosity limit and Blob viscosity limit respectively, for homogeneous emulsions.

The difference between the intrinsic viscosity predicted by the emulsion core flow model and the results of observation to hematocrit of 45% is about 20%. The monodisperse emulsion of high viscosity ratio drops is in a good qualitatively agreement with *in vivo* experiment measurements. The discrepancy is caused by the absence, in the model, of significant microcirculation characteristics such as irregularities in the microvessel wall prototype, cell aggregation, cell prototype deformation due to cell-cell interactions, leucocytes and proteins distribution in the microvessel, biconcave cell format, plasma flow through vessels wall. To fit experimental results, we suggest the analytical following equation, derived from Eq. (27)

$$\frac{\mu_s}{\mu_p} = \frac{C_1}{f_1} - C_2 \frac{f_2}{f_1^4} \epsilon + C_3 \left(\frac{f_2^2}{f_1^7} - C_4 \frac{f_3}{f_1^6} \right) \epsilon^2, \quad (33)$$

where C_i are empirical constants and have no physical meaning.

For pathologies that affects the hematocrit and cell deformation, the results of the high viscosity emulsion model permits a preliminary prediction of the intrinsic viscosity of blood by the variation of cell prototype volume fraction and λ respectively. The results in Figs. (6) and (7) would be used to predict the intrinsic viscosity of blood value in such cases.

7. ACKNOWLEDGEMENTS

Acknowledge to Capes and CNPq for providing funds to this research.

8. REFERENCES

- Barthes-Biesel, D. and Sgaier, H., 1985, Role of membrane viscosity in the orientation and deformation of a spherical capsule suspended in shear flow, "J. Fluid Mechanics", Vol. 160, pp. 119.
- Chien, S., 1987, Red cell deformability and its relevance to blood flow, "Ann. Rev. Physiology", Vol. 49, pp. 177–192.

- Cunha, F. R., 2002, Characterization of capsules and drops motion in micro-vessels for developing of models of blood flow in the microcirculation, CNPq-Report-520386.
- Cunha, F. R. and Sobral, Y. D., 2004, Characterization of the physical parameters in a process of magnetic separation and pressure-driven flow of a magnetic fluid, "Elsevier", Vol. 343, pp. 36–349.
- Evans, E. A. and Skalak, R., 1980, Mechanics and thermodynamics of biomembrane, Boca Raton, Florida.
- Fahraeus, R., 1929, Suspension stability of suspension, "Physiology", Vol. 9, pp. 241.
- Fahraeus, R. and Lindqvist, T., 1931, The viscosity of blood in narrow capillary tubes, "J. Physiology", Vol. 96, pp. 562–568.
- Frankel, N. A. and Acrivos, A., 1970, The constitutive equation for dilute emulsion, "J. Fluid Mechanics", Vol. 44, pp. 65.
- Fung, Y. C., 1973, Stochastic flow in capillary blood vessels, "Microvasc. Res.", Vol. 5, pp. 34–49.
- Hinch, J., 1997, The Viscosity of a fluid containing small drops of another fluid, "Proceedings of the Royal Society", Vol. 238, pp. 8–41.
- Lipowsky, H. H., 2005, Microvascular Rheology and Hemodynamics, "Microcirculation", Vol. 12, pp. 5–15.
- Lipowsky, H. H., Usami, S., and Chien, S., 1980, Microvascular Rheology and Hemodynamics, "Microvasc. Res.", Vol. 14, pp. 345–361.
- Mohandas, N. and Evans, E., 1998, Mechanical properties of the red cell membrane in relation to molecular structure and genetic defects, "Ann. Rev. Biophysics Biomol. Struct.", Vol. 23, pp. 787–818.
- Mohandas, N. and Shohet, 1981, The role of membrane-associated enzymes in regulation of erythrocyte shape and deformability, "Clin Haematol", Vol. 10, pp. 223–237.
- Oliveira, T. F., 2007, Microhidrodinâmica e reologia de emulsões, Doctor thesis, PUC-RJ.
- Popel, A. S. and Johnson, P. C., 2005, Microcirculation and Hemorheology, "J. Fluid Mechanics", Vol. 37, pp. 43–69.
- Pries, A. R., Neuhaus, D., and Gaehtgens, P., 1992, The viscosity of blood in narrow capillary tubes, "J. Physiology", Vol. 263, pp. H1770–78.
- Pries, A. R., Secomb, T. W., Gessner, T., Sperandio, M. B., Gross, J. F., and Gaehtgens, P., 1994, Resistance to blood flow in microvessels in vivo, "Circulation Research", Vol. 75, pp. 904–915.
- Secomb, T. W., 2005, "Biological Fluid Mechanics", Eds. C. P. Ellinton & T. J. Pedley, Company of Biologist, Cambridge.
- Secomb, T. W. and Hsu, R., 1996, Analysis of red blood cell motion through cylindrical micropores: effects of cell properties, "Biophysics J.", Vol. 71, pp. 1095.
- Secomb, T. W., Skalak, R., Ozkaya, N., and Gross, J. F., 1986, Flow of axisymmetric red blood cells in narrow capillaries, "J. Fluid Mechanics", Vol. 405, pp. 163.
- Skalak, R., Ozkaya, N., and Skalak, T. C., 1989, Biofluid mechanics, "Ann. Rev. Fluid Mechanics", Vol. 21, pp. 167.
- Sutera, S. P. and Skalak, R., 1993, The history of Poiseuille law, "J. Fluid Mechanics", Vol. 25, pp. 1–20.
- Taylor, 1932, The Viscosity of fluid Containing small drops of another fluid, "Proceedings of the Royal Society", Vol. 138, pp. 8–41.